IRAQI JOURNAL OF APPLIED PHYSICS

Fabrication and Characterization of Silver-Doped Nickel Oxide Thin Films for Gas Sensors

IJAP, Vol. (18), No. (3), July-September 2022, pp. 3-10

Qayes A. Abbas[1], Mohammed A. Hameed[2], Ahmed S. Ahmed[2]

[1] Department of Physics, College of Science, University of Anbar, Ramadi, IRAQ
[2] Department of Physics, College of Science, University of Baghdad, Baghdad, IRAQ

IRAQI JOURNAL OF APPLIED PHYSICS
Vol. 18, No. 3, July-September 2022, pp. 3-10

Fabrication and Characterization of Silver-Doped Nickel Oxide Thin Films for Gas Sensors

Qayes A. Abbas[1]
Mohammed A. Hameed[2]
Ahmed S. Ahmed[2]

[1] *Department of Physics, College of Science, University of Anbar, Ramadi, IRAQ*
[2] *Department of Physics, College of Science, University of Baghdad, Baghdad, IRAQ*

The work includes fabrication of undoped and silver-doped nanostructured nickel oxide in form thin films, which use for applications such as gas sensors. Pulsed-laser deposition (PLD) technique was used to fabricate the films on a glass substrate. The structure of films is studied by using techniques of x-ray diffraction, SEM, and EDX. Thermal annealing was performed on these films at 450°C to introduce its effect on the characteristics of these films. The films were doped with a silver element at different doping levels and both electrical and gas sensing characteristics were studied and compared to those of the undoped films. Reasonable enhancements in these characteristics were observed and attributed to the effects of thermal annealing as well as doping with silver. Gas sensing measurements were carried out using NO_2 as a gaseous species to be detected. The results showed that the electrical conductivity, density as well as mobility of charge carriers, and gas sensitivity were affected by the doping level and annealing treatment.

Keywords: Gas sensor; Nickel oxide; Nanostructures; Pulsed-laser deposition
Received: 23 March 2022; **Revised:** 13 May 2022; **Accepted:** 20 May 2022

1. Introduction

Nanomaterial oxide such as a nickel oxide (NiO) is one of the transition metal oxides that has been extensively studied in recent decades. It has physical and chemical interested properties like NaCl-like structure and antiferromagnetic oxides. As well, it has given favorable candidate for plentiful industrial applications like thermal absorber [1], photo-electrolysis [2], catalyst for oxygen evolution [3], and electrochromic equipment [4,5]. Also, NiO was well-prepared matter used in the electrodes of batteries [6,7]. The pure crystals of NiO are idealistic insulators [8,9] and many research fields have explained and resolved the insulation property of NiO [10,11]. Perceivable conductivity is done in NiO via producing Ni vacancies or substituted atoms of some alkali metals (e.g. Li) for Ni sites to fabricate rechargeable batteries [6,12]. During the last two decades, many works on doping NiO thin films with silver in atomic form have shown that such devices are highly efficient to detect very small amounts of several gaseous species as well as sunlight and electromagnetic radiation [13-16]. This multipurpose performance is not common for all similar structures.

Gas sensing applications are drastically increasing due to their industrial, environmental, and clinical importance. Meanwhile, fabrication of efficient sensors for as many as possible types of gases is the main goal of too much research works especially for gases having dangerous or harmful effects on all types of lives on the earth [17-21]. Coinciding with the revolution of nanotechnology and advanced materials, reasonable enhancements in the performance of gas sensing devices were achieved [22,23]. Amongst, metal oxide nanostructures doped with appropriate elements are dominating the industrial and environmental applications of gas sensors. Such devices can be fabricated by flexible techniques such as pulsed-laser deposition (PLD) [4,24].

The aim of this work is to study undoped and silver-doped nanostructured NiO thin films fabricated using PLD method. Both electrical and gas sensing characteristics of these structures were compared.

2. Experimental Part

The main parts of PLD technique are schematically illustrated in Fig. (1). This technique is used to prepare NiO, where the test chamber is first evacuated down to 0.001 mbar. A focused beam of Q-switched Nd:YAG laser working in the second harmonic generation (SHG) is entered the chamber through a window and directed at 45° on the surface of NiO target. The target was made as a disc from NiO nanopowder pressed as 5cm in diameter and ~2mm in thickness. One side of this disc was polished to be mirror-like. The surface of glass substrate and target surface was parallel to each other. The appropriate gap was preserved between the substrate and the used target, this makes the incident laser beam avoiding any hamper by the substrate holder. For doping experiment, silver nanopowder was mixed at different weight percentage amounts with the NiO nanopowder. The mixture was then compressed, cut and polished to form the Ag-doped NiO target. Some experimental parameters such as rotating the NiO

disc, the substrate annealing temperature and placement the target with respect to the substrate, were easily possible during the work. The structure of the prepared films was investigated using a Shimadzu 6000 X-Ray Diffractometer with Cu(kα) radiation source of 1.5406Å wavelength. The range of scanning angle (2θ) has been varied from 20 to 70 degrees and a speed of 4 deg/min. The scanning electron microscopy (SEM) and energy-dispersive x-ray spectroscopy (EDX) have been used with 15 and 10 kx magnifications.

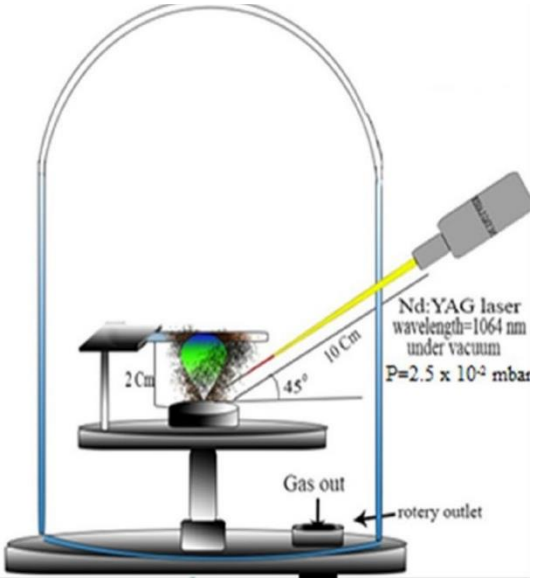

Fig. (1) Schematic diagram of main parts of PLD system [22]

Nickel oxide (NiO) powder with 99.99% purity and silver (Ag) powder with 99.9% purity were used to prepare thin films. The targets of bulk $NiO_{(1-x)}$:Ag_x have been prepared from both materials by grinding and mixing them at various concentrations (x= 0, 0.1, 0.2, 0.3 or 0.4 at.%) for 10 minutes, then pressed into pellets with 1.2 cm diameter using a SPECAC hydraulic press to apply a pressure of 6 tons/cm^2 for 10 minutes. The prepared targets of the pure NiO and Ag-doped NiO were used to prepare thin films using PLD method. Both undoped and doped samples were annealed at 450 °C using electrical furnace at atmospheric pressure for two hours for recrystallization. Thickness of the prepared films was measured using optical interferometer method. To affirm the electrical conductivity, the type of conductivity, and gas sensing measurements, interdigitated aluminum Ohmic metal contacts were deposited on the Ag:NiO films by using vacuum evaporation technique. Four-point probe (F.P.P.) method was processed on 1x1-cm^2 sheets, and for electrical properties 1mm interdigitated distance.

The experimental gas sensor system involves a test chamber of stainless steel cylinder of 15cm in diameter and 15cm in length of 15cm. This chamber contains an inlet to inflow the gas to be tested and an entry valve to inflow the atmosphere after emptying. The electrical conducting points are connected to the heater by multi-pin feedthrough at the body of the chamber. Also, sensing electrodes and thermocouples of K-type have been used. Inside this chamber, the sensor part is located upon the heater. A conductive aluminum sheet is used to connect the electrical connections of the multimeter pins with the sensor sample.

To clean the chamber from contamination, a rotary pump is used to evacuate it down to about 1 mbar. A temperature controller is used to set the gas sensor at the required temperature. Finally, to measure the change in resistance, a PC-interfaced digital multimeter is used. These processes are repeated for all operation temperatures.

3. Results and Discussion

Figure (2) represents the XRD pattern of the sample annealed at 450°C for two hours. It showed that the planes (111), (200), and (220) correspond to angles of 32.9°, 43.7°, and 63.0° respectively, which are matched with the JCPDS file 73-1523 [25]. Also, it is found that the prepared structure is quadrilateral and polycrystalline.

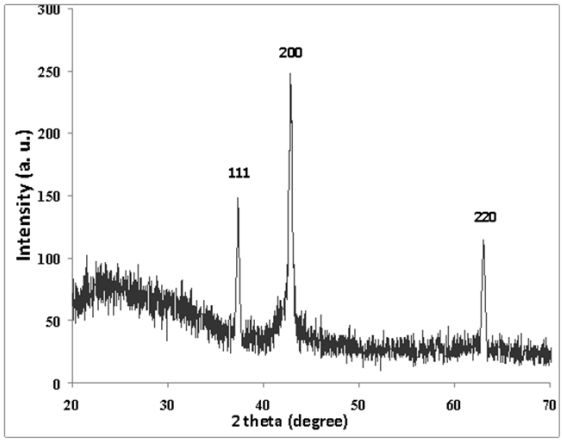

Fig. (2) XRD pattern of 3% Ag:NiO sample annealed at 450°C for two hours

Figure (3) shows SEM images and EDX result for 3% Ag-doped NiO thin film. The SEM images are shown that the particles have several morphologies. They have different tiny asymmetrical nano-size clusters. Furthermore, the sample has various grain sizes ranging from 50 to 500 nm. The EDX is carried out to determine the elemental composition of the film sample. It emphasizes in a qualitative mode the presence of oxygen (O), silicon (Si), nickel (Ni), and silver (Ag) atoms that compose the sample.

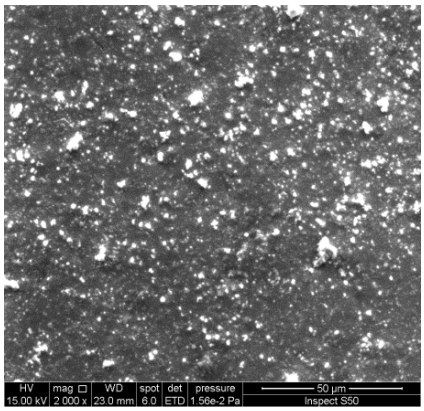

(a)

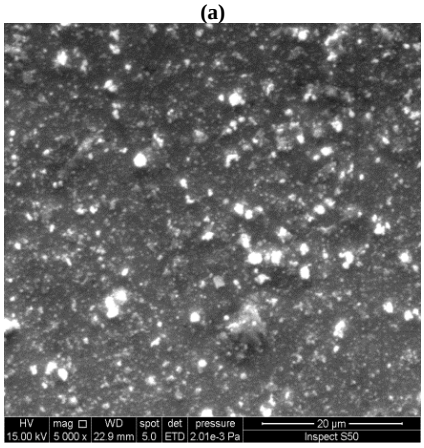

(b)

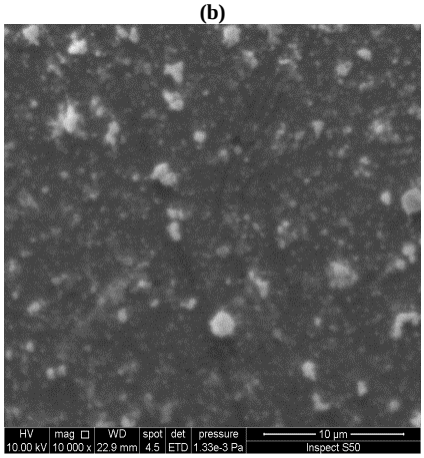

(c)

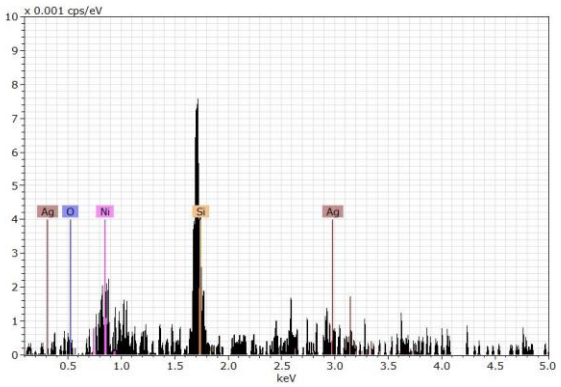

Fig. (3) SEM and EDX results for 3% Ag-doped NiO thin film prepared by PLD technique. SEM result is presented in three magnification scales (50, 20 and 10 µm)

Figure (4) exhibits the variation of the electrical conductivity (Lnσ) with the reciprocal temperature (1000/T) of as-prepared and annealed NiO thin films of both types (undoped and Ag-doped). Thermal annealing was performed at 450°C in order to induce the structural distribution of NiO grains over the prepared thin films. This thermal annealing may have another effect to enhance the substitutional doping of NiO structure with Ag atoms. Both effects were compared to the as-prepared undoped NiO samples. It is clear that increasing temperature causes the electrical conductivity to increase as the charge carriers are provided with higher kinetic energy to move and generate electrical signal with higher intensity. Similarly, higher level of doping with silver causes the electrical conductivity to increase as more silver atoms contribute to the electrical conduction of the doped NiO sample. Doping level of 4% has increased the electrical conductivity of both as-prepared and annealed samples by 150% when compared to the undoped sample.

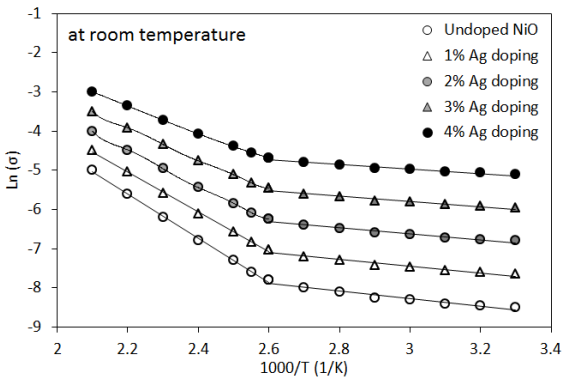

(a)

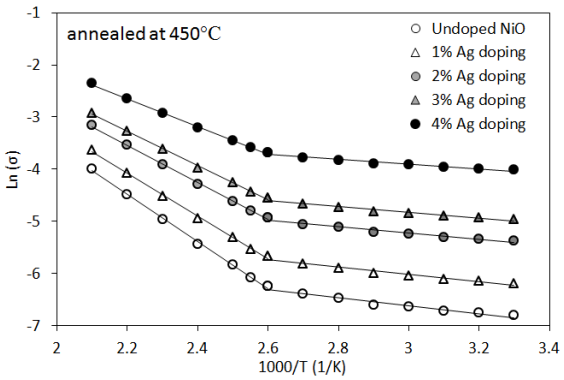

(b)

Fig. (4) Variation of Ln(σ) with 1000/T for undoped and Ag-doped NiO samples (a) as-prepared (at room temperature) and (b) annealed at 450°C

Variety of mechanisms can be used to explain the electrically conductive behavior of polycrystalline NiO thin films. Extrinsic impurities are giving the ability to grow in impurity conduction behavior at depressed temperatures and band conduction close to and higher than the room temperature. The grain boundary works as shipping traps, controlling the potential barriers and barriers throughout the grain, which makes the electric conductivity of these films

influenced [26,27]. Additionally, when the semiconductor is at low temperatures, or heavily doped, the dominated current of band conduction is caused by emitted thermal-field of the carriers through the barrier, and at high temperatures or in lightly doped material, thermionic emission dominates over the barrier [28-30]. These processes are taken into account in the analysis of the electrical transport properties of prepared samples in the present study.

The Hall measurements showed that pure and Ag-doped NiO thin film samples are p-type semiconductors. For p-type samples, the Hall parameters involve the electrical conductivity (σ), Hall effect coefficient (R_H), carrier concentration (n_H), and mobility (μ_H).

At room temperature, the electrical conductivity (σ_{RT}) of the annealed samples was determined and compared to that of as-prepared samples, as shown in Fig. (5). The effects of silver doping ratio as well as thermal annealing are very clear, as the electrical conductivity was increased by 36.4% at silver doping ratio of 4% compared to the as-prepared sample doped at the same ratio, while an increase of 23.8% was determined at doping ratio of 1% compared to the as-prepared sample doped at the same level. So, increasing the Ag doping level by 400% has resulted in a consequent increase in the electrical conductivity of about 13%. As the doping ratio is increased, additional dopant atoms occupy sites of Ni atoms in NiO lattice and result in increasing charge carriers. The essential objective of doping NiO crystalline structure with silver is to produce more charge carriers and thus increasing the electrical signal during the response to the tested gas.

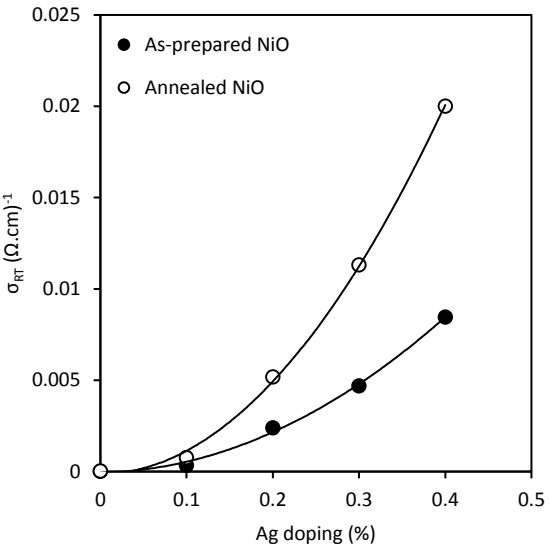

Fig. (5) Variation of room-temperature electrical conductivity (σ_{RT}) with Ag doping level (%) for as-prepared and annealed (at 450°C) NiO thin films

The variation in the density of charge carriers with doping level was determined as shown in Fig. (6). It was observed that the average increase in the density of charge carriers of Ag-doped NiO samples due to thermal annealing was about 79% when compared to the as-prepared Ag-doped NiO samples. Thermal annealing allows Ag atoms to substitute Ni atoms in the NiO structure much more effectively and thus additional charge carriers are provided and the electrical conduction is increased. However, thermal annealing has resulted in an increase of 200% leading to arise in the density of charge carriers for the undoped NiO films.

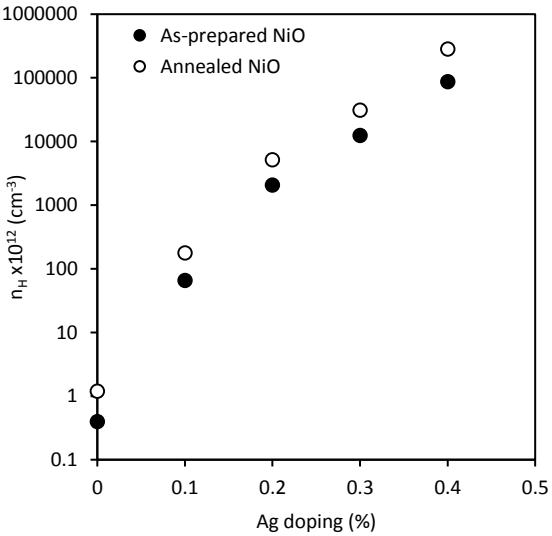

Fig. (6) Variation of carrier concentration (n_H) as a function of Ag doping level (%) for as-prepared and annealed (at 450°C) NiO thin films

Figure (7) shows the variation of mobility (μ_H) with percentage doping level for both as-prepared and annealed samples. The thermal annealing of the pure NiO sample affects the mobility of the charge carriers by increasing it by 145%. In existence of Ag dopants, the mobility was slightly decreased. High dopant concentration leads to the ionized impurity scattering from the substitutional donors and scattering from the interstitials [31,32], resulting in a decrease in the mobility.

The aggregate variation that occurs in the mobility and density of charge carriers can be demonstrated as the position of Ag dopants in the NiO structure. The mobility of charge carriers was reduced at the higher doping concentrations which could be resulted from the interstitial occupancy of Ag atoms in NiO structure. The appearance of Ag dopants at interstitial sites and grain boundaries in oxide form, and diminishing grain size, may act as scattering centers and lead to a remarkable decrease in the mobility at a high dopant concentration. From this result, one may conclude that low doping level of NiO with Ag atoms improves the conductivity of the film as the electrical conductivity of Ag element is higher than that of NiO.

The prepared samples have been tested as sensors to detect the harmful NO_2 gas at different operation temperatures. The sensitivity (S) is determined by the following equation [33]:

$$S = \left|\frac{R_g - R_a}{R_a}\right| \times 100\% \qquad (1)$$

where R_a and R_g are the electric resistances of the samples in air and in existence of tested gas, respectively

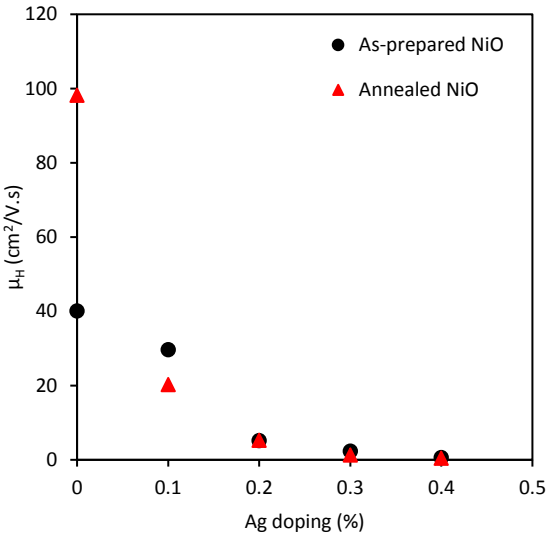

Fig. (7) Variation of mobility (μ_H) with Ag doping level (%) for as-prepared and annealed (at 450°C) NiO thin films

Figure (8) illustrates the variation of resistance of Ag-doped NiO thin films to NO_2 gas at operation temperature for different measurement times (30, 60 and 90 min). The resistance has been increased as the operation temperature reaches to 200°C for measuring times of 30 and 60 min, while the maximum resistance was reached at 260°C for measuring time of 90 min. The two behaviors were identical, which means that the Ag-doped NiO samples as gas sensors work preferably at elevated temperatures in comparison with those at lower temperatures (<200°C). However, further increase in operation temperature led to decrease the sensitivity of these devices.

In order to introduce the effect of doping with silver on the performance of the fabricated gas sensors, the resistance of undoped and Ag-doped NiO samples has been tested with time. From this figure, the mechanism of a variable resistance depends on the time before exposing the NiO samples to NO_2 gas. The system was left to stabilize at its operation temperature for about 15 min, thus the stabilized resistance is assigned as R_a (Gas_{on}). During exposing the sample to the NO_2 gas, the resistance is reduced and assigned as R_g (Gas_{off}). The species of NO_2 gas react with oxygen ions on the surface of the sample and therefore, the oxidation mechanism leads to rising the quantity of the free carriers. Thus, the resistance of the samples reduces when exposed to oxidant gases.

The sensitivity was measured at higher operation temperatures as presented in Fig. (9). The sensitivity of prepared films is growing with increasing operation temperature to 200°C. The vibration of NiO molecules and the speed of gas diffusion are increased as a result of increasing the temperature and this results in gas adsorption. The desorption rate of the sample's surface raises and thus the sensitivity is increased according to the increase in the temperature. The higher sensitivity of Ag-doped NiO samples achieved in this work was about ~79% at an operation temperature of 200°C.

Furthermore, the required parameters to design the gas sensing devices include the response time, which is the time required for the sensor to realize 90% of the maximum variation in resistance in the presence of the detected gas. Another considerable parameter is the recovery time, which can be denoted as the time required to go back to 10% of the higher resistance of the sensor device. These two parameters were tested at a bias voltage of 6 V. All results in table (1) for both parameters are decreased according to increasing the operation temperature when sensing NO_2 gas.

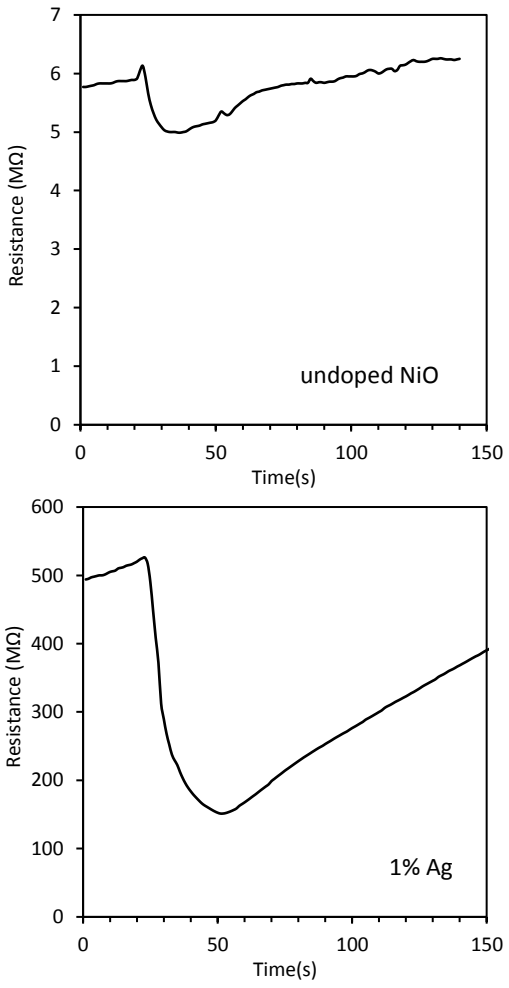

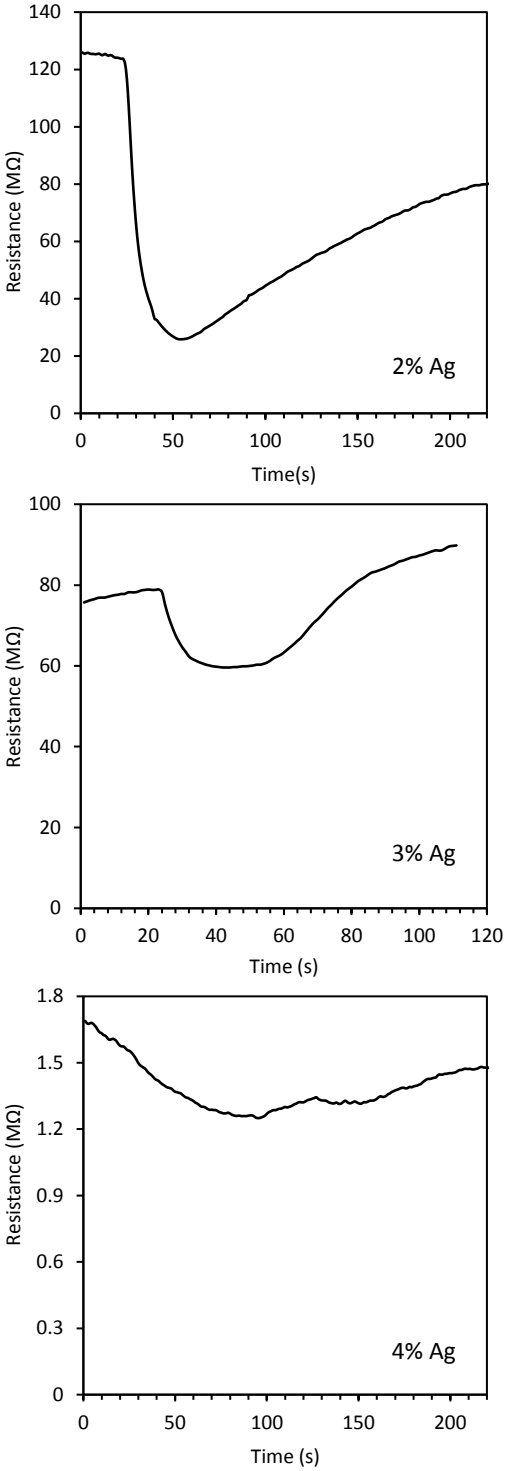

Fig. (8) Variation of thin film sample resistance (R) with time for annealed (at 450°C) undoped and Ag-doped NiO thin films at operation temperature of 200°C

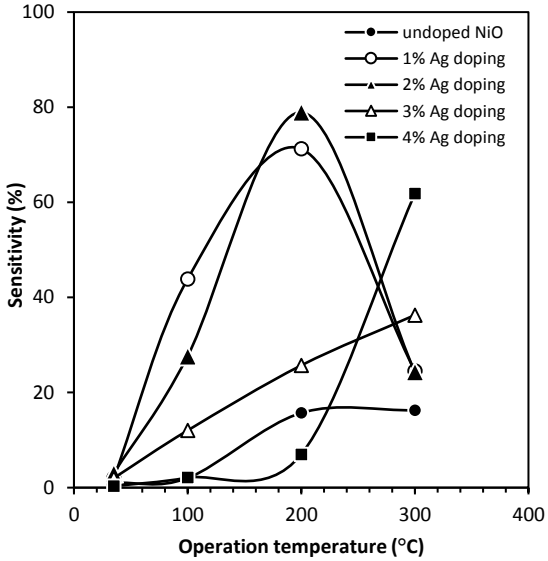

Fig. (9) Variation of sensitivity of Ag-doped NiO thin films to NO_2 gas with operation temperature for different measurement times

Table (1) Results of response time and recovery time of Ag-doped NiO thin film gas sensors at different operation temperatures

T (°C)	Undoped NiO		1% Ag doping		2% Ag doping	
	Response time (s)	Recovery time (s)	Response time (s)	Recovery time (s)	Response time (s)	Recovery time (s)
35	-	-	-	-	-	-
100	25.2	221.4	31.5	216.9	42.3	117.9
200	26.1	133.2	25.2	134.1	14.4	56.7
300	19.8	49.5	19.8	58.5	36	76.5

T (°C)	3% Ag doping		4% Ag doping	
	Response time (s)	Recovery time (s)	Response time (s)	Recovery time (s)
35	32.4	216	-	-
100	29.7	126.9	24.3	89.1
200	35.1	97.2	25.2	61.2
300	27.9	84.6	9.9	60.3

4. Conclusion

In concluding remarks, pulsed-laser deposition was used to prepare Ag-doped NiO thin films. These films were thermally annealed at 450°C and their electrical characteristics were affected by the Ag doping levels. Doping level of 4% has increased the electrical conductivity of both as-prepared and annealed samples by 150%. The average increase in the density and mobility of charge carriers of Ag-doped NiO samples due to thermal annealing were about 79% and 145%, respectively. The overall variation in the density and mobility of charge carriers can be interpreted according to the position of Ag atoms within the NiO crystalline structure. The Ag-doped NiO thin film gas sensors operate better at

elevated temperatures when compared to the lower temperatures (<200°C). The maximum gas sensitivity of Ag-doped NiO samples was ~79% at operation temperature of 200°C.

Acknowledgment

Authors would like to acknowledge the University of Baghdad and the University of Anbar for their support to this work.

References

[1] J. Huang and Q. Wan, "Gas Sensors Based on Semiconducting Metal Oxide One-Dimensional Nanostructures", Sensors, 9 (2009) 9903-9924.

[2] O.A. Hamadi, N.J. Shakir and F.H. Hussain, "Magnetic Field and Temperature Dependent Measurements of Hall Coefficient in Thermal Evaporated Tin-Doped Cadmium Oxide Thin Films", Bulg. J. Phys., 37(4) (2010) 223-231.

[3] M.D. Irwin et al., "Structural and electrical functionality of NiO interfacial films in bulk heterojunction organic solar cells", Chem. Mater., 23 (2011) 2218-2226.

[4] P. Mallick and N.C. Mishra, "Evolution of structure, microstructure, electrical and magnetic properties of nickel oxide (NiO) with transition metal ion doping", Am. J. Mater. Sci., 2(3) (2012) 66-71.

[5] B.S. Kwak et al., "Synthesis of spherical NiO nanoparticles using a solvothermal treatment with acetone solvent", J. Indust. Eng. Chem., 18 (2012) 11-15.

[6] A.M. Soleimanpour, A.H. Jayatissa and G. Sumanasekera, "Surface and gas sensing properties of nanocrystalline nickel oxide thin films", Appl. Surf. Sci., 276 (2013) 291-297.

[7] G. Zhang et al., "Synthesis of one-dimensional hierarchical NiO hollow nanostructures with enhanced supercapacitive performance", Nanoscale, 5 (2013) 877-881.

[8] M. Barman, S. Paul and A. Sarkar, "Electronic properties in Mn doped and pure NiO clusters", Proc. Int. Conf. on Recent Trends in Appl. Phys. Mater. Sci. (RAM 2013), Bikaner, Rajasthan, India, 1-2, (2013) 427-428.

[9] Y.A. Kumar Reddy, A. Sivasankar Reddy and P. Sreedhara Reddy, "Influence of oxygen partial pressure on the physical properties of Ag doped NiO thin films", Proc. Int. Conf. on Recent Trends in Appl. Phys. Mater. Sci. (RAM 2013), Bikaner, Rajasthan, India, 1-2, (2013) 475-476.

[10] S.H. Faisal and M.A. Hameed, "Heterojunction Solar Cell Based on Highly-Pure Nanopowders Prepared by DC Reactive Magnetron Sputtering", Iraqi J. Appl. Phys., 16(3) (2020) 27-32.

[11] R.H. Turki and M.A. Hameed, "Spectral and Electrical Characteristics of Nanostructured NiO/TiO_2 Heterojunction Fabricated by DC Reactive Magnetron Sputtering", Iraqi J. Appl. Phys., 16(3) (2020) 39-42.

[12] J.W. Jung, C.-C. Chueh and A.K.-Y. Jen, "A Low-Temperature, Solution-Processable, Cu-Doped Nickel Oxide Hole-Transporting Layer via the Combustion Method for High-Performance Thin-Film Perovskite Solar Cells", Adv. Mater., 27(47) (2015) 7874-7880.

[13] X. Wang and Z. Wei, "Optical Properties of Silver Doped NiO Films Prepared by Spray Pyrolysis Method", J. Adv. Microsc. Res., 10(1) (2015) 24-27(4).

[14] A.V. Kadu, S.V. Jagtap and N.N. Gedam, "Preparation and Gas Sensing Performance of Nanostructured Copper Doped Nickel Oxides", Int. J. Chem. Phys. Sci., 4 (2015) 186-194.

[15] O.A. Hammadi, M.K. Khalaf and F.J. Kadhim, "Fabrication of UV Photodetector from Nickel Oxide Nanoparticles Deposited on Silicon Substrate by Closed-Field Unbalanced Dual Magnetron Sputtering Techniques", Opt. Quantum Electron., 47(12) (2015) 3805-3813.

[16] M.A. Hameed, S.H. Faisal and R.H. Turki, "Characterization of Multilayer Highly-Pure Metal Oxide Structures Prepared by DC Reactive Magnetron Sputtering Technique", Iraqi J. Appl. Phys., 16(4) (2020) 25-30

[17] J.A. Dirksen, K. Duval and T.A. Ring, "NiO thin-film formaldehyde gas sensor", Sen. Actuat. B: Chem., 80(2) (2001) 106-115.

[18] I. Hotovy et al., "Sensing characteristics of NiO thin films as NO_2 gas sensor", Thin Solid Films, 418 (1) (2002) 9-15.

[19] X.H. Xia et al., "Electrochromic properties of porous NiO thin films prepared by a chemical bath deposition", Solar Energy Mater. Solar Cells, 92 (2008) 628-633.

[20] B. Varghese et al., "Fabrication of NiO nanowall electrodes for high performance lithium ion battery", Chem. Mater., 20 (2008) 3360-3367.

[21] M. Stamataki et al., "Hydrogen gas sensors based on PLD grown NiO thin film structures", phys. Stat. sol. a, 205(8) (2008) 2064-2068.

[22] I. Simon et al., "Selected gas response measurements using reduced graphene oxide decorated with nickel nanoparticles", Nano Mater. Sci., 3 (2021) 412-419

[23] B. Sowmya, J. Athira and P.K. Panda, "A review on metal-oxide based p-n and n-n heterostructured nano-materials for gas sensing applications", Sens. Int., 2 (2021) 100085.

[24] O.A. Hamadi, "Characteristics of CdO-Si Heterostructure Produced by Plasma-Induced Bonding Technique", Proc. IMechE, Part L, J. Mater.: Design & Appl., 222 (2008) 65-71.

[25] H.E. Swanson et al., **"Standard X-ray Diffraction Powder Patterns"**, US Dept. Commerce, NBS sec. 1 (1962) 47.

[26] O. Kingsley et al., "Efficient p-type doping of sputter-deposited NiO thin films with Li, Ag, and Cu acceptors", Phys. Rev. Mater., 4 (2020)

104603.
[27] Y. Wei et al., "Improving the efficiency and environmental stability of inverted planar perovskite solar cells via silver-doped nickel oxide hole-transporting layer", Appl. Surf. Sci., 427(B) (2018) 782-79.
[28] A.S. Ahmed and M.A. Hameed, "Widening of the optical band gap of $CdO_{2(1-X)}Al_{(X)}$ thin films prepared by pulsed laser deposition", Appl. Phys. A, 127 (2021) 188.
[29] M.T. Ramesan and V. Santhi, "Synthesis, characterization, conductivity and sensor application study of polypyrrole/silver doped nickel oxide nanocomposites", Composite Interfaces, 25 (8) (2018) 725-741.
[30] X. Xia et al., "Lithium and Silver Co-Doped Nickel Oxide Hole-Transporting Layer Boosting the Efficiency and Stability of Inverted Planar Perovskite Solar Cells", ACS Appl. Mater. Interfaces, 10(51) (2018) 44501-44510.
[31] J. Zheng et al., "Solution-Processed, Silver-Doped NiOx as Hole Transporting Layer for High-Efficiency Inverted Perovskite Solar Cells", ACS Appl. Energy Mater., 1(2) (2018) 561-570.
[32] O.A. Hammadi and N.E. Naji, "Fabrication and Characterization of Polycrystalline Nickel Cobaltite Nanostructures Prepared by Plasma Sputtering as Gas Sensor", Phot. Sen., 8(1) (2018) 43-47.
[33] I.M. Ali et al. "Structural, Optical and Sensing Behavior of Neodymium-Doped Vanadium Pentoxide Thin Films", Iranian J. Sci. Technol. Trans. Sci., 42 (2018) 2375-2386.